Electronic Supporting Information to:

Heterobimetallic contacts in statistical co-crystals of homoleptic coordination compounds with ligand-encoded H···F bonds:

Structure, photophysics and mechano-responsive properties

Tobias Theiss,[a,b] Stefan Buss, [a,b] Iván Maisuls, [a,b] Theresa Block,[a] Jutta Kösters,[a] Rainer Pöttgen,[a] and Cristian A. Strassert[a,b]

[a] Institut für Anorganische und Analytische Chemie, Universität Münster, Corrensstraße 28/30, 48149 Münster, Germany

[b] CiMIC, SoN, CeNTech, Universität Münster, Heisenbergstraße 11, 48149 Münster, Germany

Correspondence to: Prof. C. A. Strassert – eMail: ca.s@uni-muenster.de

Table of Contents

Section S1: Methods and materials

The pure compounds [**PtL**] and [**PdL**] were synthesized as reported.[1] To obtain the corresponding statistical co-crystals, [**PtL**] and [**PdL**] were dissolved in DCM in the ratios 3:1, 1:1, and 1:3 (n:n) and the solvent was slowly evaporated.

S1.1 X-ray diffraction measurements on single crystals

The X-ray diffraction measurements for the crystalline samples (100 K data) were carried out at the Institut für Anorganische und Analytische Chemie (Universität Münster) using a Venture single crystal X-ray diffractometer (Bruker AXS, Karlsruhe, Germany). The X-ray diffractometric data reduction was carried out using *SAINT+*.[2] The crystal structures were solved by using *SHELXTL*.[3] The molecular structures in the crystal and the unit cells were created with *MERCURY*.[4] All details of the crystallographic data for the above-mentioned compounds are available from the Cambridge Crystallographic Data Center (CCDC) using the corresponding depository number (2300665, 2303661, 2303662). The basic crystallographic data is summarized in Table S1. The relevant atomic positions, occupancy parameters and the displacement parameters for the metal sites are listed in Tables S2 and S3. All further details are documented within the CIF files.

The single crystals selected from the sample with the 1:1 ratio of [**PtL**] and [**PdL**] had good quality. During the structure refinement we could refine the atomic positions of the metal sites along with their displacement parameter without constraints. Contrarily, even after several cycles of re-crystallization and different methods, it was not possible to obtain crystals of similar quality for the 3:1 and 1:3 ratios. The statistical distribution of the Pt(II) and Pd(II) ions caused problems with the electron density. For these refinements the Pt and Pd displacement parameters had to be coupled to similar values. The underlying category A and B alerts are explained in the CIF files. This is a consequence of the [**PtL**] / [**PdL**] disorder. Nevertheless, we could reliably refine these structures and draw a consistent picture with respect to the [**PtL**] / [**PdL**] arrangements.

Micro X-ray fluorescence spectroscopy (μXRF). To investigate the elemental ratio on the crystals' surfaces, a laboratory benchtop μXRF spectrometer M4 Tornado (Bruker Nano GmbH, Berlin, Germany) was used. The Rh-anode micro-focus X-ray tube was set at a voltage of 50 kV and anode current of 600 μA. The device is equipped with polycapillary optics to focus the incident X-ray beam on a size of 29 μm for the Mo-K-alpha line and was evacuated to 20 mbar, to eliminate interference

caused by the argon atmosphere. The analytes Ca ($K_{\alpha1}$ = 3.692 keV), Pd ($L_{\alpha1}$ = 2.837 keV) and Pt ($L_{\alpha1}$ = 9,442 keV) were detected on their major K- or L-alpha lines. The signals were detected by means of a silicon drift detector (SDD, XFlash® 5030, Bruker Nano GmbH). Data processing was performed using the software ESPRIT HyperMap (Bruker Nano GmbH).

S1.2 Photoluminescence spectroscopy

Steady-state excitation and emission spectra were recorded on a FluoTime 300 spectrometer from PicoQuant equipped with a 300 W ozone-free Xe lamp (200-1100 nm), a 10 W Xe flash-lamp (200-1100 nm, pulse width ca. 1 µs) with repetition rates of 1-300 Hz, a double-grating excitation monochromator (Czerny-Turner type, grating with 1200 lines/mm, blaze wavelength: 300 nm), diode lasers (pulse width < 20 ps) operated by a computer-controlled laser driver PDL-820 “Sepia II” (repetition rate up to 80 MHz, burst mode for slow and weak decays), two emission monochromators (Czerny-Turner, selectable between double-grating blazed at 500 nm with 2.7 nm/mm dispersion and 1200 lines/mm, or single-grating blazed at 1250 nm with 5.4 nm/mm dispersion and 600 lines/mm) with adjustable slit width between 25 µm and 7 mm, Glan-Thompson polarizers for excitation (after the Xe-lamps) and emission (after the sample). Different sample holders (Peltier-cooled mounting unit ranging from -15 to 110 °C or an adjustable front-face sample holder), along with two detectors (namely a PMA Hybrid-07 from PicoQuant with transit time spread FWHM < 50 ps, 220-850 nm, or a H10330C-45-C3 NIR detector with transit time spread FWHM 0.4 ns, 950-1400 nm from Hamamatsu) were used. Steady-state spectra and photoluminescence lifetimes were recorded in TCSPC mode by a PicoHarp 300 (minimum base resolution 4 ps) or in MCS mode by a TimeHarp 260 (where up to several ms can be traced). Emission and excitation spectra were corrected for source intensity (lamp and grating) by standard correction curves. For samples with lifetimes in the ns order, an instrument response function calibration (IRF) was performed using a diluted Ludox® dispersion. Lifetime analysis was performed using the commercial EasyTau 2 software (PicoQuant). The quality of the fit was assessed by minimizing the reduced chi squared function ($\chi2$) as well as visual inspection of the weighted residuals and their autocorrelation. All solvents used were of spectrometric grade (Uvasol®, Merck).

Time-resolved multiphoton micro(spectro)scopy was performed using a fluorescence microscope (IX 73 from Olympus) equipped with a complete confocal system, a laser combining unit (LCU), an inverted microscope body, and a multichannel detection unit (MultiHarp 150, PicoQuant) equipped with diode lasers. These lasers provide adjustable output power and repetition rates up to 80 MHz, all within a compact fiber-coupled unit with wavelengths ranging from 375 to 640 nm). A FLIMbee galvo scanner is positioned between the main optical unit (MOU) and the microscope to achieve extremely stable

scanning speeds while maintaining high positioning precision, enabling applications ranging from fast fluorescence lifetime imaging (rapidFLIM) to phosphorescence lifetime imaging measurements (PLIM).

For beam diagnostics, a charge-coupled device (CCD) camera and a photodiode are available in the MOU of the microscope. The MOU is equipped with two detectors: a hybrid photomultiplier-based single-photon counting module (PMA Hybrid 40, PicoQuant) and a SPAD-based photon counting module (SPCM-AQR-14, Perkin-Elmer). Depending on the emission of the sample, various band-pass (BP) and low-pass (LP) filters were placed in front of these detectors as needed to acquire lifetime maps. Data acquisition was conducted using the unique time-tagged time-resolved (TTTR) measurement mode, allowing for simultaneous data acquisition on two channels. The data was processed and analyzed with the SymphoTime 64 (PicoQuant) software.

To couple the MicroTime 200 and the FluoTime 300 instruments, a fiber coupler was employed, enabling the spectrometer to record either steady-state or time-resolved luminescence spectra and decays from a sample mounted on the microscope. Luminescence micrographs were acquired using the aforementioned microscope, equipped with a X-CiteQ Lamp module (Excelitas Technologies) as the excitation source and a UI-5580SE (IDS) digital camera. Depending on the photophysical properties of the sample, different band pass (BP) and low pass (LP) cubes were used accordingly.

Section S2: X-ray diffraction data of the complexes in single crystals

Table S1. μXRF-analysis of the statistical co-crystals. Each row within a sample represents a different crystal. As a consequence of the variable crystal tilt, the standard deviation is *ca*. 5 atom percent. For each composition, three independent crystals were analyzed (five point measurements for each crystal).

Sample	%Pt	%Pd
[**PtL**][**PdL**] 3:1	70	30
	63	37
	74	26
[**PtL**][**PdL**] 1:1	61	39
	61	39
	64	36
[**PtL**][**PdL**] 1:3	41	59
	42	58
	37	63

Table S2: Single crystal data and structure refinement details for the [**PtL**][**PdL**] crystals of compositions 3:1, 1:1 and 1:3, space group *C*2/*c*, *Z* = 8 (100 K data).

Co-crystal	[**PtL**][**PdL**] 3:1	[**PtL**][**PdL**] 1:1	[**PtL**][**PdL**] 1:3
Empirical formula	$C_{34}H_{29}F_4N_5O_2Pd_{0.26}Pt_{0.74}$	$C_{34}H_{29}F_4N_5O_2Pd_{0.51}Pt_{0.49}$	$C_{34}H_{29}F_4N_5O_2Pd_{0.73}Pt_{0.27}$
Molar mass, g mol^{-1}	787.21	765.15	746.19
Lattice parameters, Å	a = 34.00(3)	a = 33.6105(6)	a = 33.95(4)
(single crystal data)	b = 13.44(1)	b = 13.3921(2)	b = 13.27(3)
	c = 13.77(1)	c = 13.4561(3)	c = 13.845(9)
Monoclinic angle, °	β = 107.54(6)	β = 106.0890(10)	β = 106.92(9)
Cell volume, nm^3	V = 6.002	V = 5.8196	V = 5.968
Calculated density, g cm^{-3}	1.80	1.75	1.71
Crystal size, μm^3	28 × 64 × 240	23 × 260 × 270	16 × 160 × 300
Diffractometer type	Bruker Venture	Bruker Venture	Bruker Venture
Radiation/wavelength, pm	MoK_α / 71.073	MoK_α / 71.073	MoK_α / 71.073
Transmission (max / min)	0.901 / 0.463	0.941 / 0.523	0.971 / 0.607
Abs. coefficient, mm^{-1}	3.8	2.7	1.8
F(000), e	3116	3052	2998
ϑ range, deg	2.15-30.34	2.16-31.00	2.15-27.87
hkl range	±44; ±17; ±17	±44; ±17; ±17	±44; ±17; ±17
Total no. reflections	31364	71719	34315
Indep. reflections / R_{int}	6923 / 0.0459	6944 / 0.0181	6931 / 0.0578
Refl. with $I > 3\sigma(I)$ / R_σ	5206 / 0.0705	5944 / 0.0473	4394 / 0.0888
Data/parameters	6923 / 422	6944 / 429	6931 / 422
Goodness-of-fit on F^2	1.11	1.11	1.06
$R1$/$wR2$ for $I > 3\sigma(I)$	0.0761 / 0.2115	0.0484 / 0.1373	0.0775 / 0.2082
$R1$/$wR2$ for all data	0.0947 / 0.2321	0.0551 / 0.1434	0.1179 / 0.2455
Extinction coefficient	–	0.00100(13)	–
Larg. diff. peak/hole, e Å^{-3}	3.63 / –3.49	1.54 / –1.63	2.88 / –2.32
CCDC number	2300665	2303661	2303662

Table S3. Coordinates (Wyckoff sites 8*f* in space group *C*2/*c*) and occupancy parameters for the metal positions (freely refined) of the three different statistical co-crystals.

Atom	*x*	*y*	*z*	occupancy / %
[PtL][PdL] sample ratio of 1:3				
Pd	0.4826(6)	0.7057(12)	0.3609(12)	72.8(8)
Pt	0.4842(8)	0.7045(16)	0.3629(17)	27.2
[PtL][PdL] sample ratio of 1:1				
Pd	0.48332(4)	0.70561(16)	0.36133(14)	51.4(6)
Pt	0.48329(3)	0.70529(7)	0.36155(6)	48.6
[PtL][PdL] sample ratio of 3:1				
Pd	0.5192(9)	0.701(2)	0.640(2)	26.6(11)
Pt	0.51627(15)	0.7062(4)	0.6384(4)	73.4

Table S4. Anisotropic displacement parameters (pm^2) for the metal positions of the three different statistical co-crystals. The data quality allowed only a decoupled refinement for the **[PtL][PdL]** 1:1 crystal, while the displacements were constrained for the remaining to data sets.

Atom	U_{11}	U_{22}	U_{33}	U_{12}	U_{13}	U_{23}
[PtL][PdL] sample ratio of 1:3						
Pd	759(12)	287(4)	429(5)	4(3)	149(6)	10(5)
Pt	759(12)	287(4)	429(5)	4(3)	149(6)	10(5)
[PtL][PdL] sample ratio of 1:1						
Pt	587(9)	191(6)	248(5)	2(3)	215(5)	3(3)
Pd	209(8)	359(18)	458(16)	2(8)	–38(6)	10(6)
[PtL][PdL] sample ratio of 3:1						
Pt	485(8)	265(6)	422(4)	–1(3)	113(5)	2(4)
Pd	485(8)	265(6)	422(4)	–1(3)	113(5)	2(4)

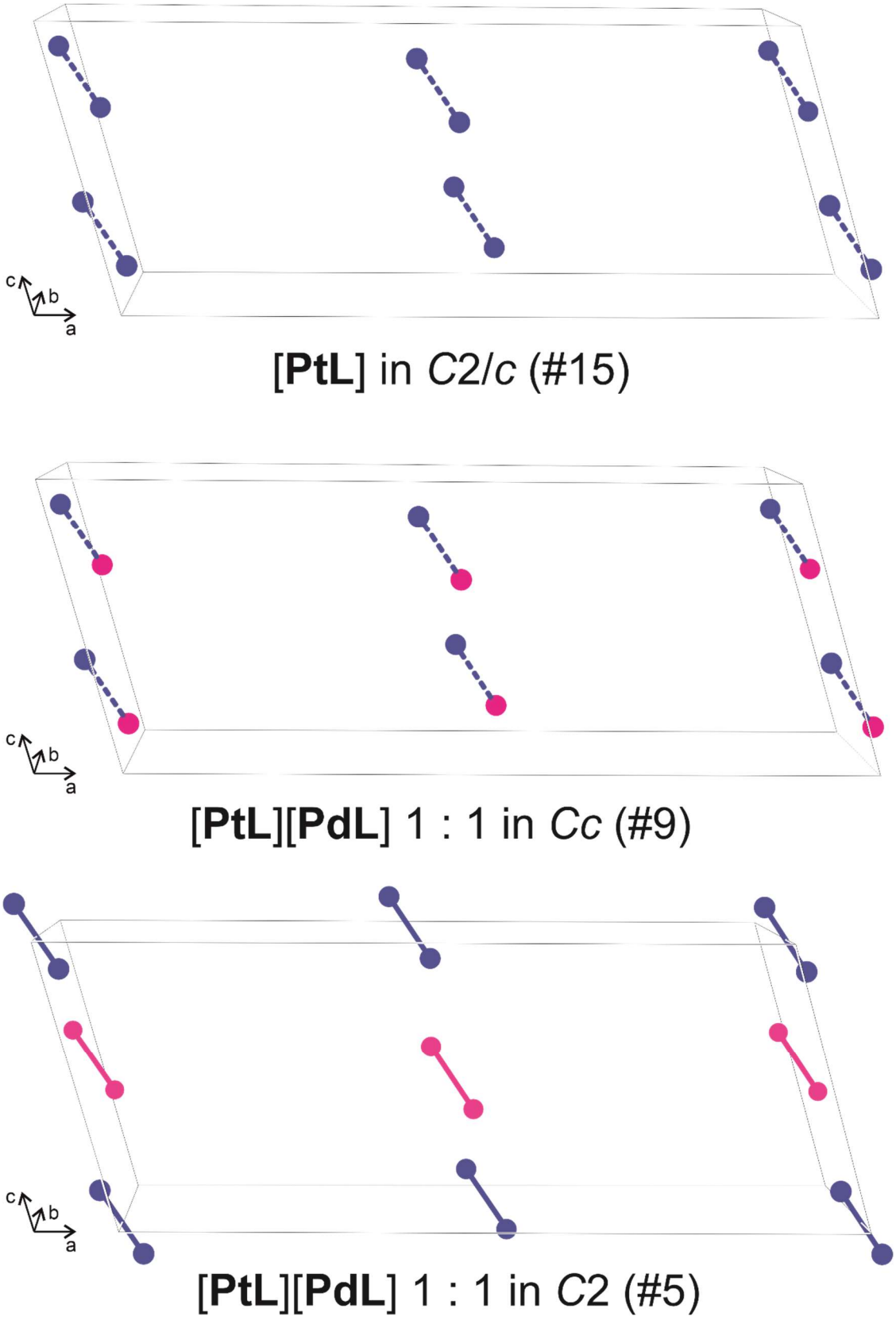

Fig. S1. Ordering possibilities of the platinum and palladium atoms in co-crystals of [**PtL**] and [**PdL**]. The pure platinum and palladium compounds crystallize with the centrosymmetric monoclinic space group *C*2/*c*. A 1:1 [**PtL**][**PdL**] co-crystal can show platinum-palladium ordering only in the non-centrosymmetric ordering variants in space groups *Cc* (#9; ordered Pt–Pd dumb-bells) and *C*2 (#5; ordered Pt_2 and Pd_2 dumb-bells). Note that the symmetry reduction from *C*2/*c* to *C*2 deserves a shift of 0 0 1/4.

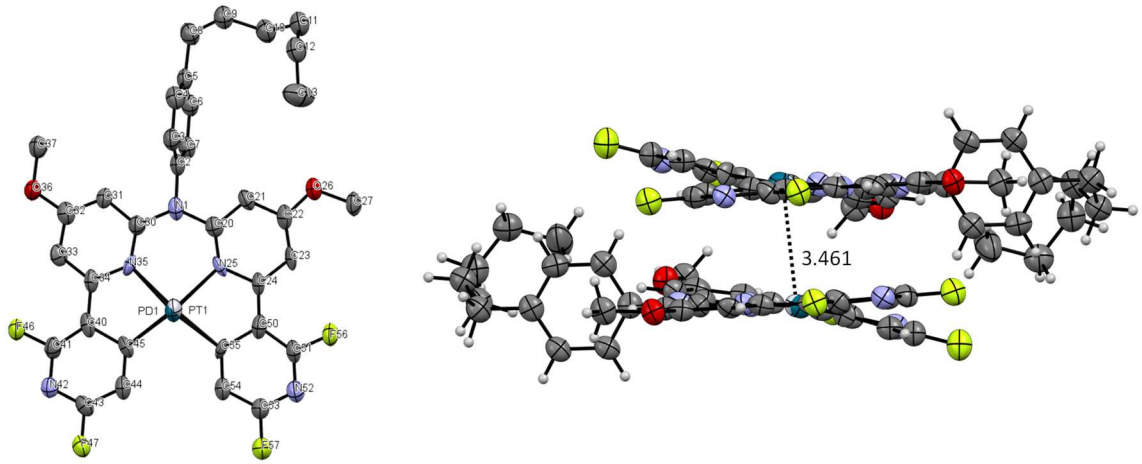

Fig. S2. Left: Molecular structure in the single crystal for [**PtL**][**PdL**] 3:1 with labelled atoms. Hydrogen atoms have been omitted for clarity. Right: Dimeric structure for [**PtL**][**PdL**] 3:1 with metal-metal-distance given in Ångstrom (Å). Displacement ellipsoids are shown at 50% probability. A micrograph of the crystal is shown in Figure S24.

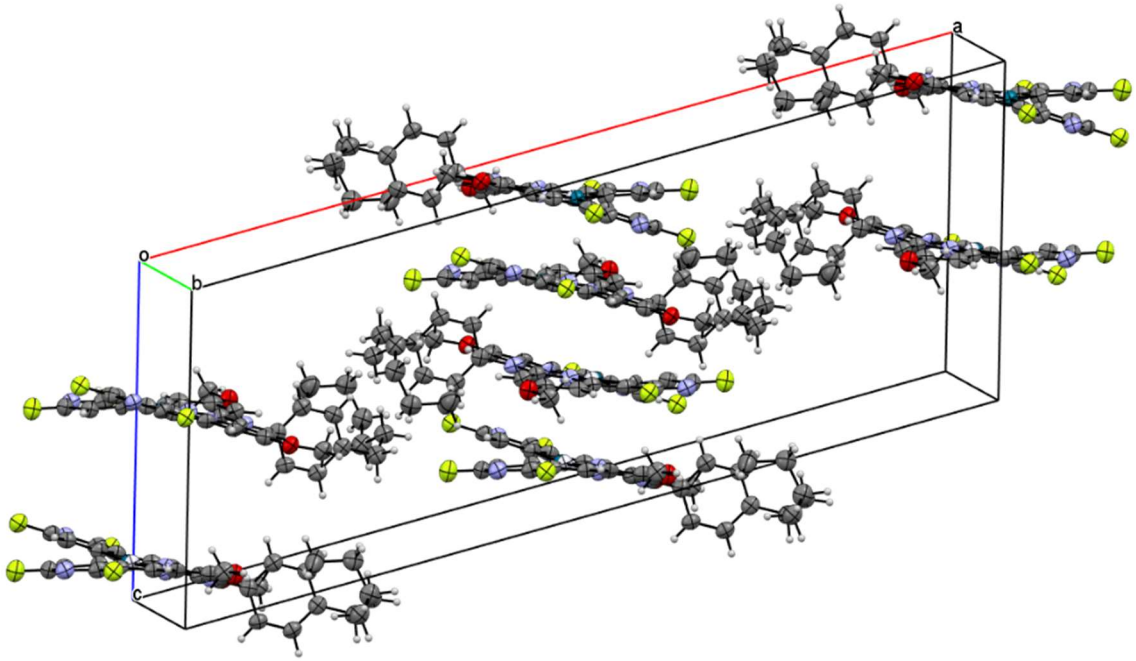

Fig. S3. Unit cell for [**PtL**][**PdL**] 3:1. Displacement ellipsoids are shown at 50% probability.

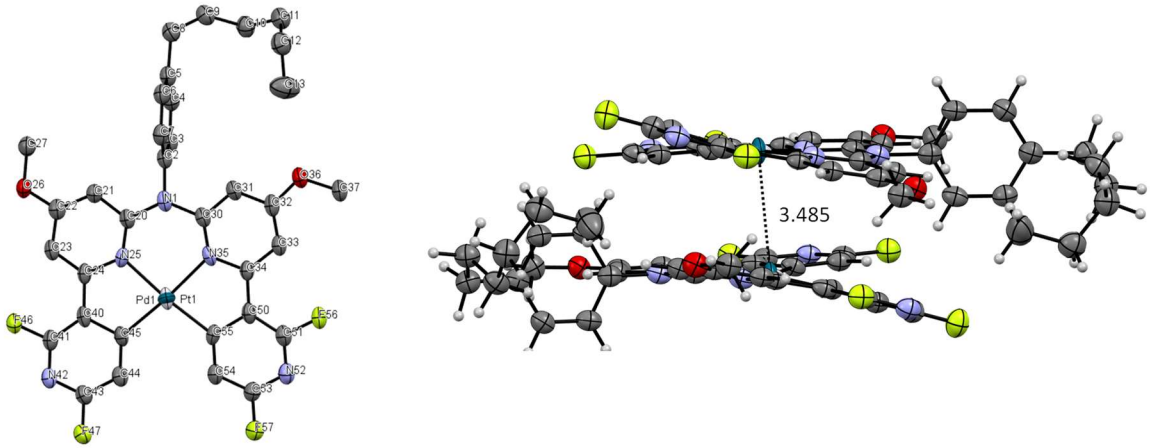

Fig. S4. Left: Molecular structure in the single crystal for [**PtL**][**PdL**] 1:1 with labelled atoms. Hydrogen atoms have been omitted for clarity. Right: Dimeric structure for [**PtL**][**PdL**] 1:1 with metal-metal-distance given in Ångstrom (Å). Displacement ellipsoids are shown at 50% probability. A micrograph of the crystal is shown in Figure S24 and Figure S25.

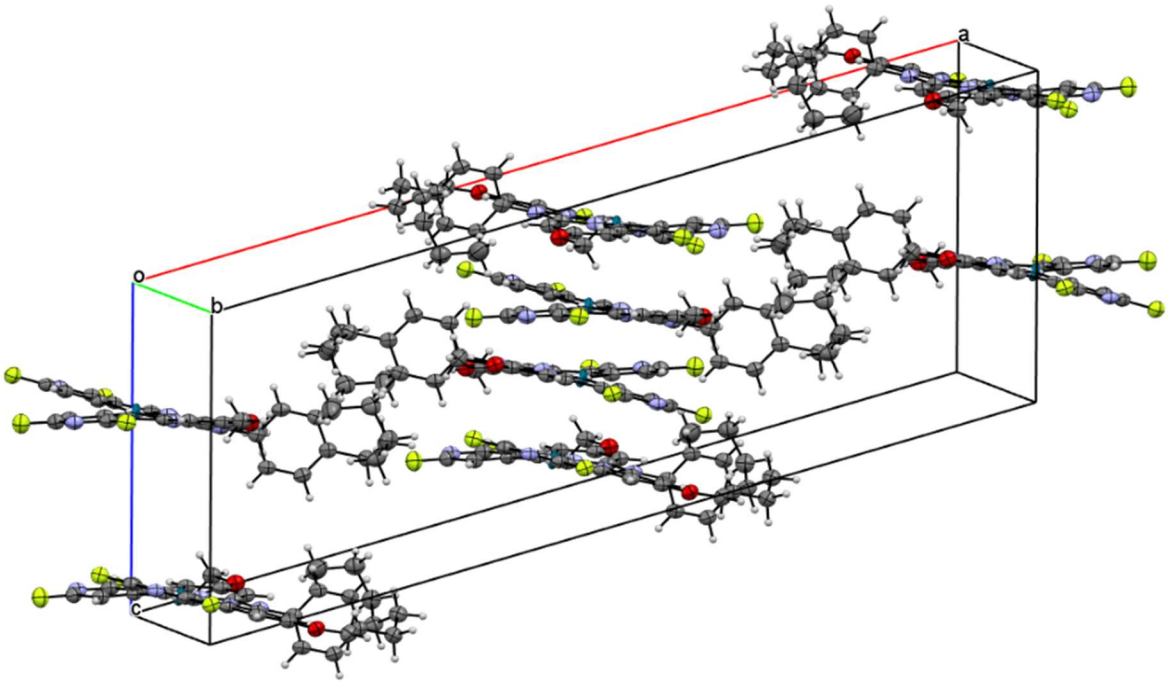

Fig. S5. Unit cell for [**PtL**][**PdL**] 1:1. Displacement ellipsoids are shown at 50% probability.

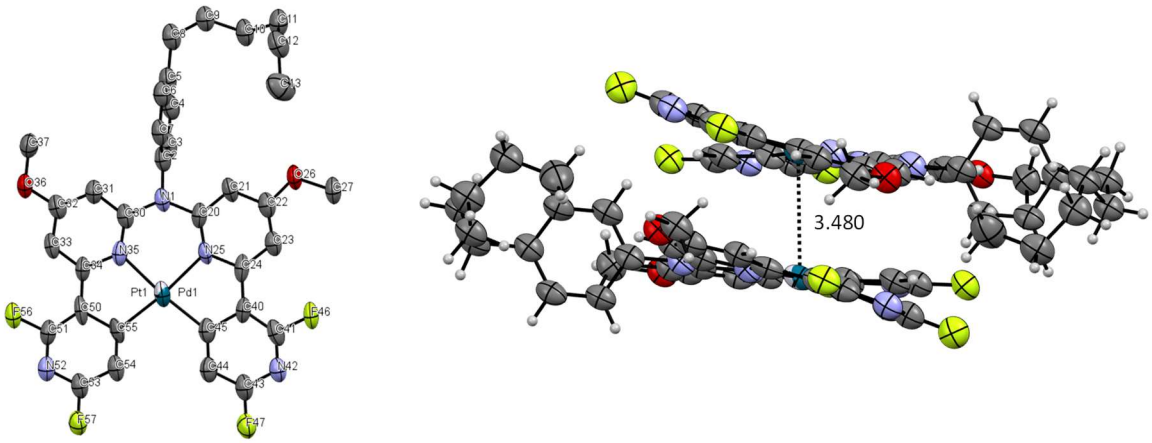

Fig. S6. Left: Molecular structure in the single crystal for [**PtL**][**PdL**] 1:3 with labelled atoms. Hydrogen atoms have been omitted for clarity. Right: Dimeric structure for [**PtL**][**PdL**] 1:3 with metal-metal-distance given in Ångstrom (Å). Displacement ellipsoids are shown at 50% probability. A micrograph of the crystal is shown in Figure S24.

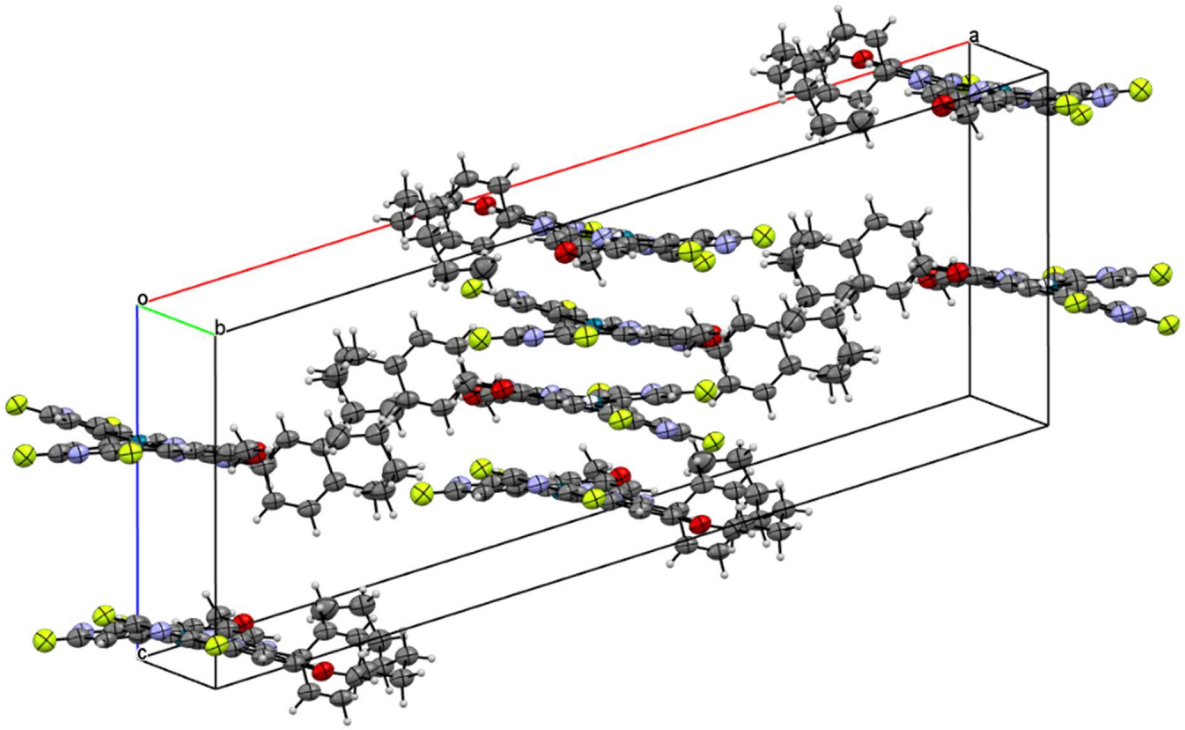

Fig. S7. Unit cell for [**PtL**][**PdL**] 1:3. Displacement ellipsoids are shown at 50% probability.

Section S3: Photophysical characterization

Table S5. Summarized photophysical data of the statistical co-crystals in different conditions.

Compound	Medium	λ_{em} / nm	λ_{exc} / nm
[**PtL**][**PdL**] 1:1	DCM, $c = 1 \cdot 10^{-3}$ M, air-equilibrated, 298 K	720	375
		600	375
		465	375
		750	375
		650	375
		465	375
	DCM/MeOH 1:1, $c = 1 \cdot 10^{-5}$ M, glassy matrix, 77 K	460	375
		540	375
		670	375
	crystal	590	375
	ground solid	610	375
[**PtL**][**PdL**] 1:3	DCM/MeOH 1:1, $c = 1 \cdot 10^{-5}$ M, glassy matrix, 77 K	460	375
		550	375
		630	375
	crystal	580	375
	ground solid	600	375
[**PtL**][**PdL**] 3:1	DCM/MeOH 1:1, $c = 1 \cdot 10^{-5}$ M, glassy matrix, 77 K	460	405
		540	405
		590	405
		680	405
	crystal	580	375
	ground solid	610	375

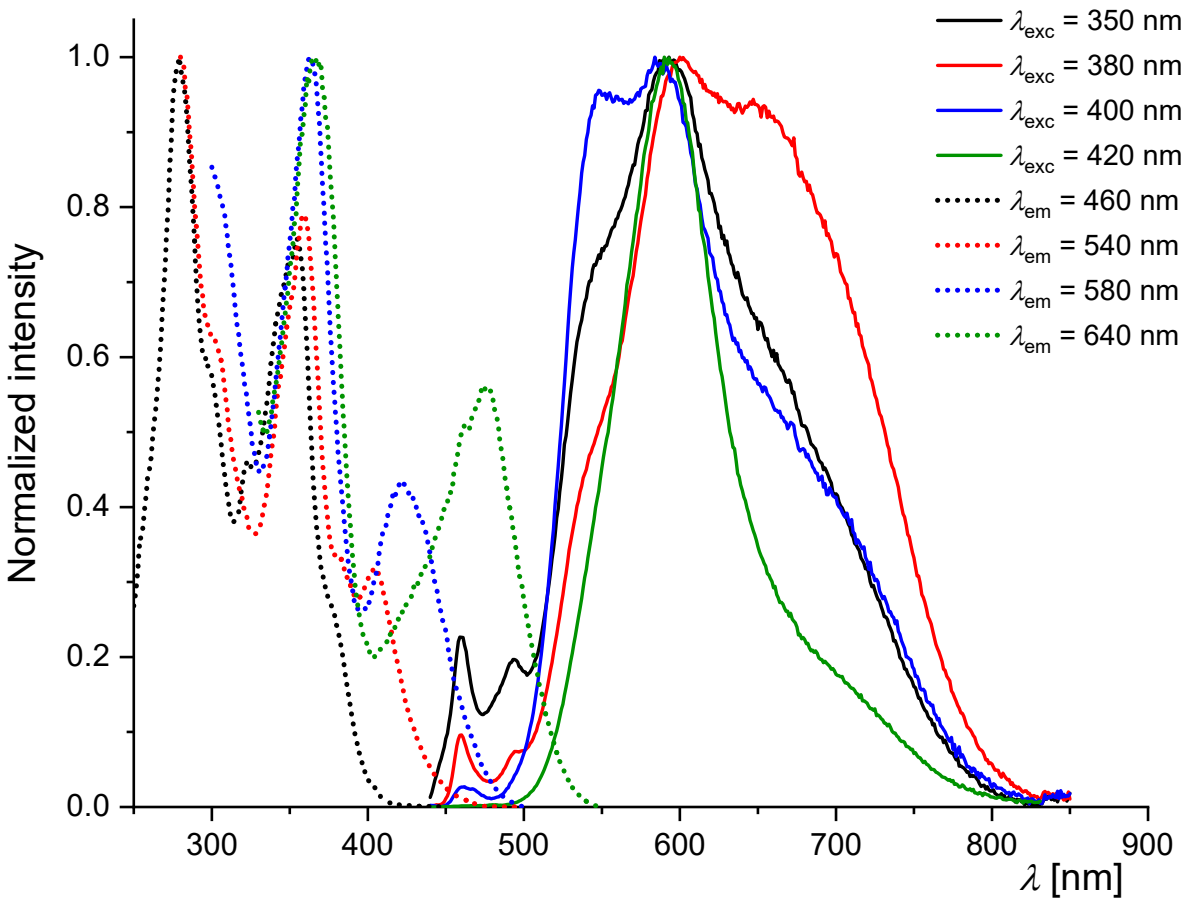

Fig. S8. Excitation (dotted lines; black: λ_{em} = 460 nm; red: λ_{em} = 540 nm; blue: λ_{em} = 580 nm; green: λ_{em} = 640 nm) and emission spectra (solid lines; black: λ_{exc} = 350 nm; red: λ_{exc} = 380 nm; blue: λ_{exc} = 400 nm; green: λ_{exc} = 420 nm) of [**PtL**][**PdL**] 3:1 at 77 K in a frozen glassy matrix of DCM/MeOH (V:V = 1:1). $c = 1 \cdot 10^{-5}$ M. Spectra normalized to the highest intensity.

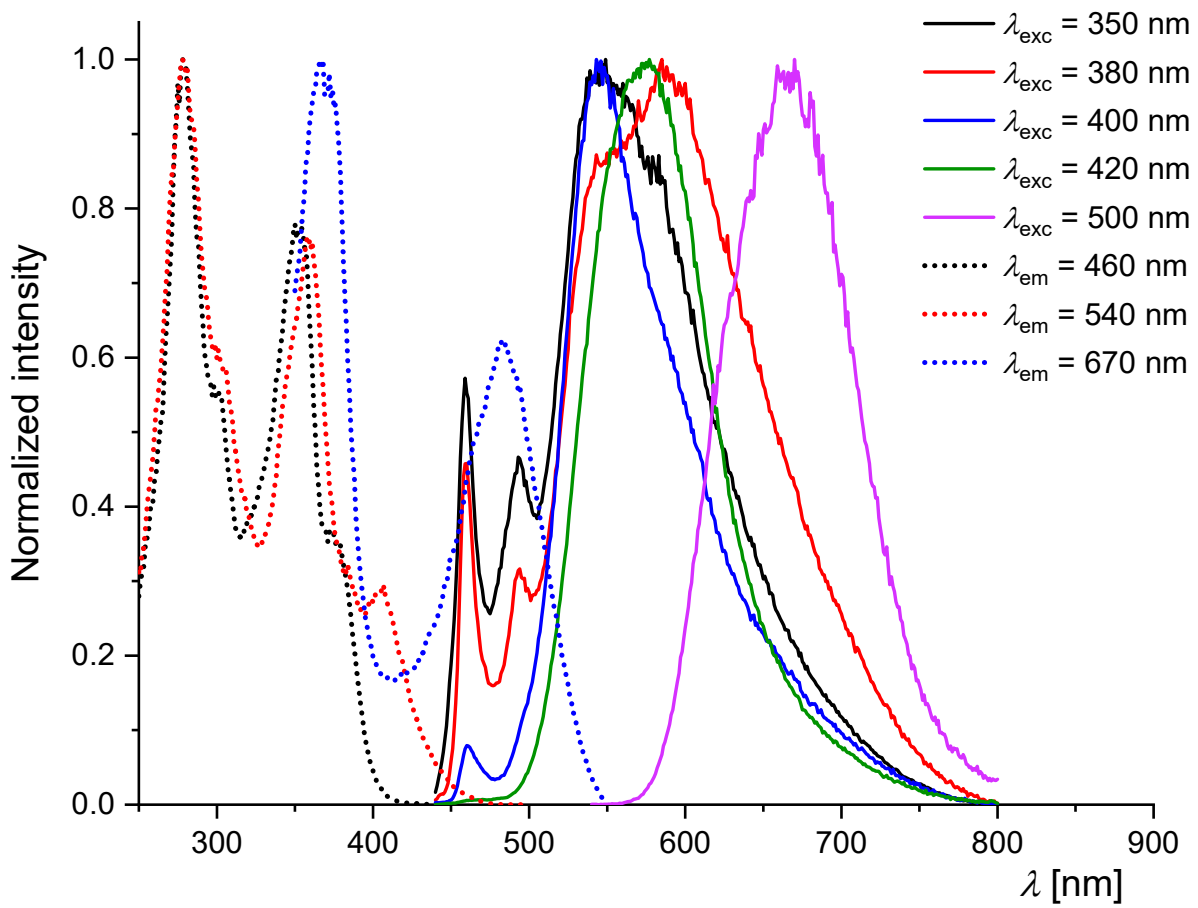

Fig. S9. Excitation (dotted lines; black: λ_{em} = 460 nm; red: λ_{em} = 540 nm; blue: λ_{em} = 670 nm) and emission spectra (solid lines; black: λ_{exc} = 350 nm; red: λ_{exc} = 380 nm; blue: λ_{exc} = 400 nm; green: λ_{exc} = 420 nm; magenta: λ_{exc} = 500 nm) of [**PtL**][**PdL**] 1:1 at 77 K in a frozen glassy matrix of DCM/MeOH (V:V = 1:1). c = $1 \cdot 10^{-5}$ M. Spectra normalized to the highest intensity.

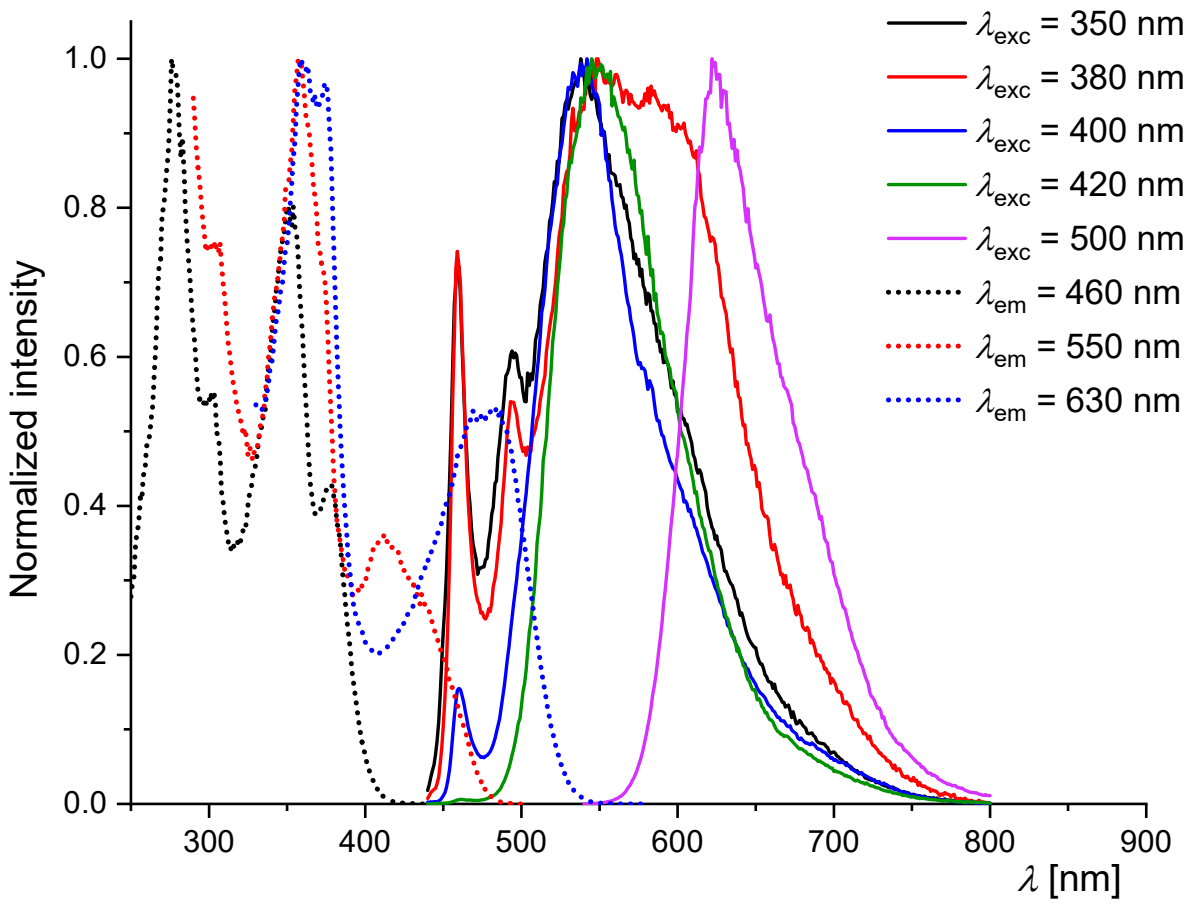

Fig. S10. Excitation (dotted lines; black: λ_{em} = 460 nm; red: λ_{em} = 550 nm; blue: λ_{em} = 630 nm) and emission spectra (solid lines; black: λ_{exc} = 350 nm; red: λ_{exc} = 380 nm; blue: λ_{exc} = 400 nm; green: λ_{exc} = 420 nm; magenta: λ_{exc} = 500 nm) of [**PtL**][**PdL**] 1:3 at 77 K in a frozen glassy matrix of DCM/MeOH (V:V = 1:1). $c = 1 \cdot 10^{-5}$ M. Spectra normalized to the highest intensity.

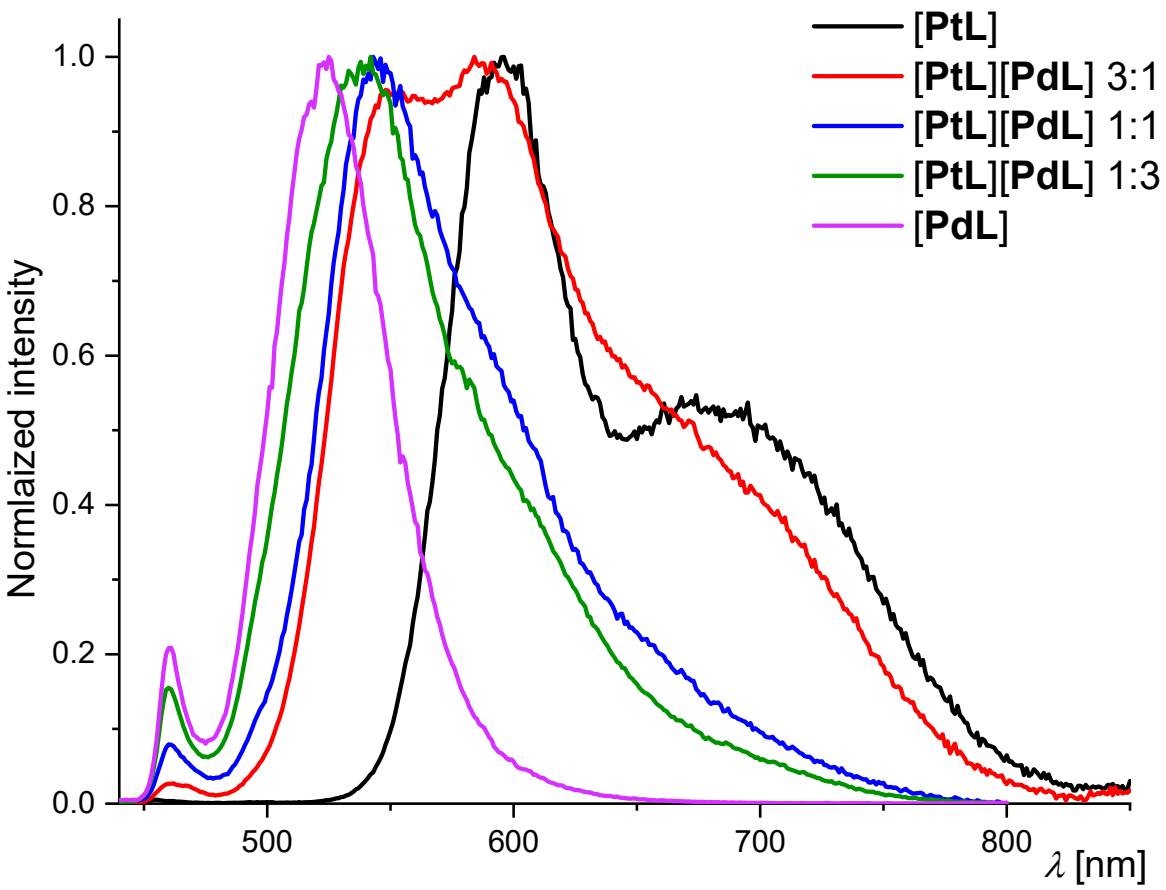

Fig. S11. Emission spectra (λ_{exc} = 400 nm) of [**PtL**] (black), [**PtL**][**PdL**] 3:1 (red), [**PtL**][**PdL**] 1:1 (blue), [**PtL**][**PdL**] 1:3 (green), [**PdL**] (magenta) at 77 K in a frozen glassy matrix of DCM:MeOH (V:V = 1:1). c = $1 \cdot 10^{-5}$ M. Spectra normalized to the highest intensity.

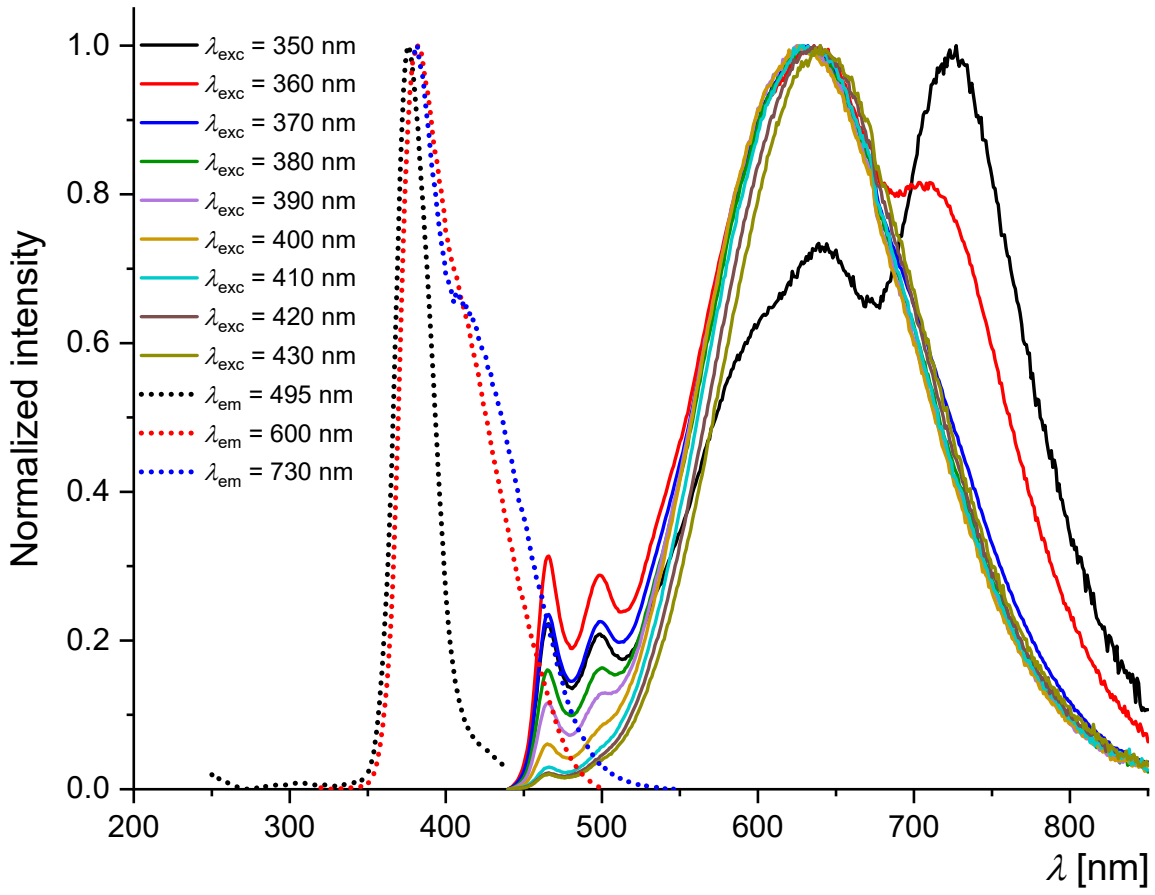

Fig. S12. Excitation (dotted lines; black: λ_{em} = 495 nm; red: λ_{em} = 600 nm; blue: λ_{em} = 730 nm) and emission spectra (solid lines, black: λ_{exc} = 350 nm; red: λ_{exc} = 360 nm; blue: λ_{exc} = 370 nm; green: λ_{exc} = 380 nm; magenta: λ_{exc} = 390 nm; ocher: λ_{exc} = 400 nm; cyan: λ_{exc} = 410 nm; brown: λ_{exc} = 420 nm; ocher-green: λ_{exc} = 430 nm) of [**PtL**][**PdL**] 1:1 in liquid air-equilibrated DCM solutions at 298 K. $c = 1 \cdot 10^{-3}$ M. Spectra normalized to the highest intensity.

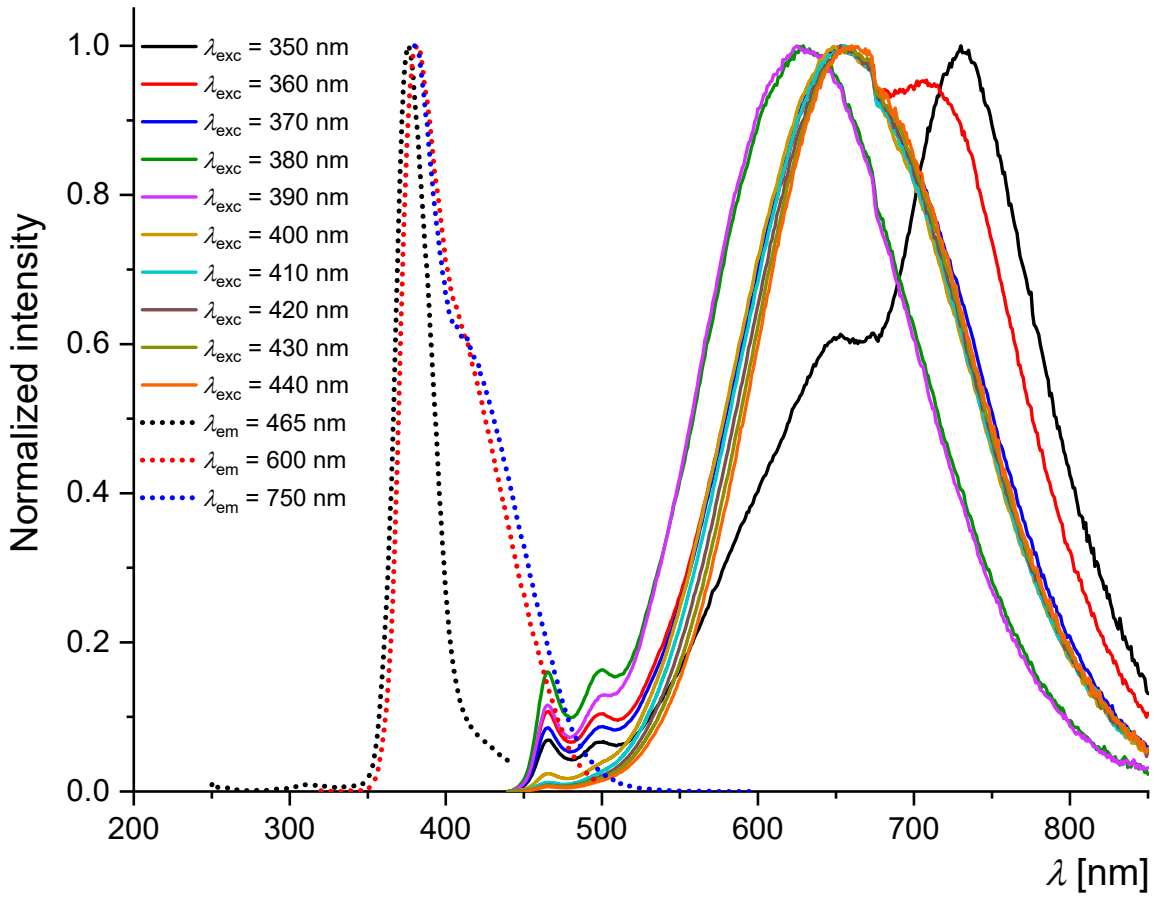

Fig. S13. Excitation (dotted lines; black: λ_{em} = 495 nm; red: λ_{em} = 600 nm; blue: λ_{em} = 750 nm) and emission spectra (solid lines; black: λ_{exc} = 350 nm; red: λ_{exc} = 360 nm; blue: λ_{exc} = 370 nm; green: λ_{exc} = 380 nm; magenta: λ_{exc} = 390 nm; ocher: λ_{exc} = 400 nm; cyan: λ_{exc} = 410 nm; brown: λ_{exc} = 420 nm; ocher-green: λ_{exc} = 430 nm; orange: λ_{exc} = 440 nm) of [**PtL**][**PdL**] 1:1 in liquid Ar-purged DCM solutions at 298 K. $c = 1 \cdot 10^{-3}$ M. Spectra normalized to the highest intensity.

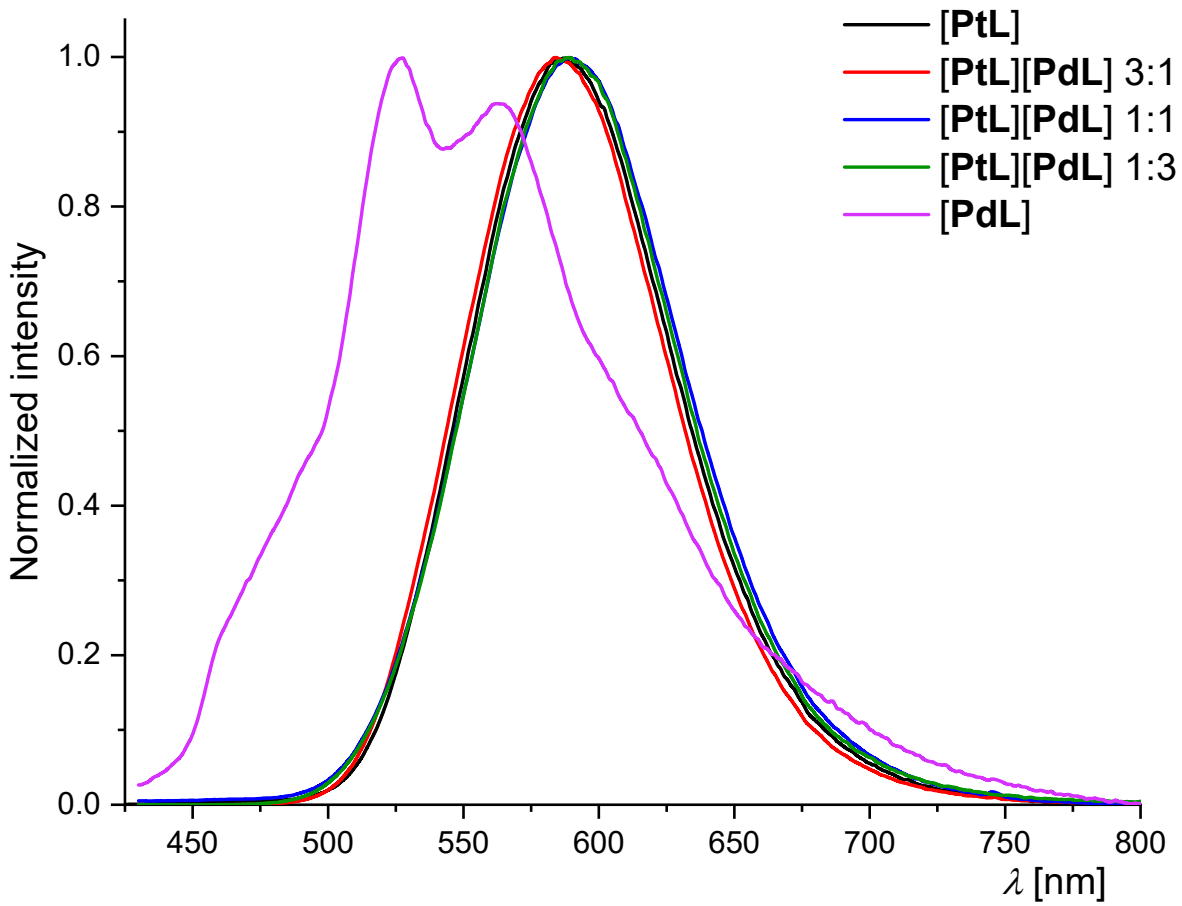

Fig. S14. Emission spectra (λ_{exc} = 376 nm) of [**PtL**] (black), [**PtL**][**PdL**] 3:1 (red), [**PtL**][**PdL**] 1:1 (blue), [**PtL**][**PdL**] 1:3 (green), [**PdL**] (magenta) as crystalline solids at 298 K. Spectra normalized at the highest intensity (acquired using a front-face sample holder in a photoluminescence spectrometer).

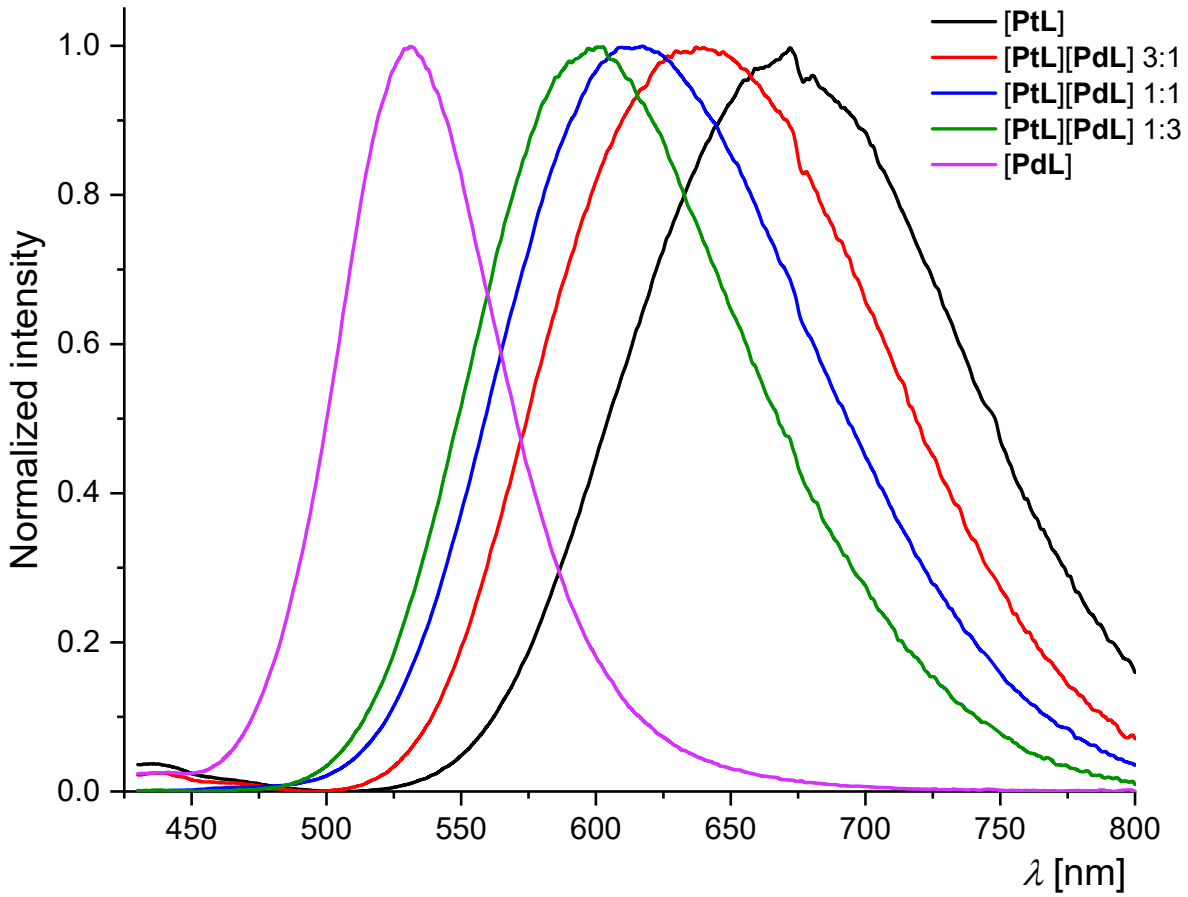

Fig. S15. Emission spectra (λ_{exc} = 376 nm) of [**PtL**] (black), [**PtL**][**PdL**] 3:1 (red), [**PtL**][**PdL**] 1:1 (blue), [**PtL**][**PdL**] 1:3 (green), [**PdL**] (magenta) as ground solids at 298 K. Spectra normalized at the highest intensity (acquired using a front-face sample holder in a photoluminescence spectrometer).

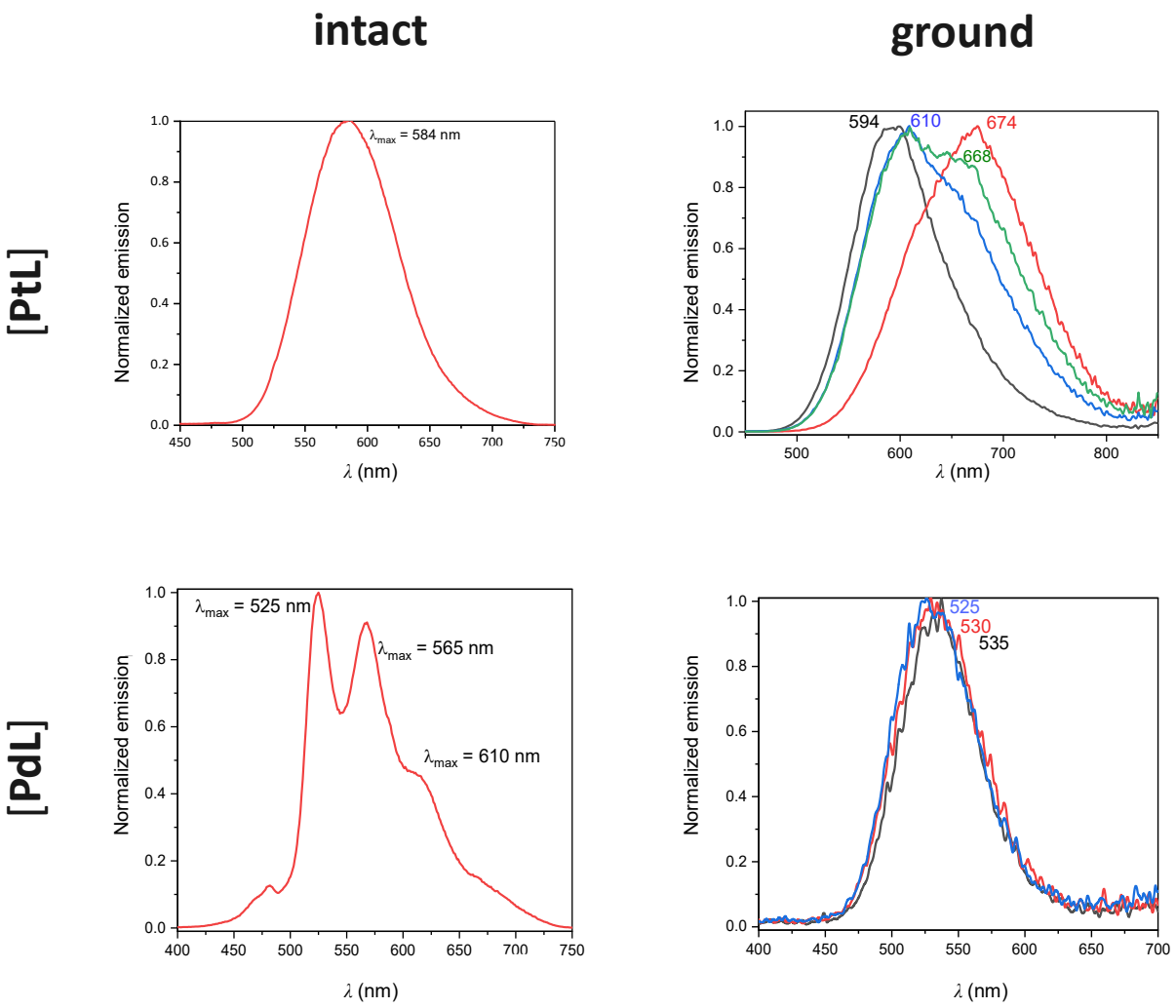

Fig. S16. Photoluminescence spectra (λ_{ex} = 375 nm) of the pure complexes [**PtL**] and [**PdL**] in the crystalline state before (left) and after (right) mechanical grinding; recorded using time-resolved photoluminescence micro(spectro)scopy. The spectra of the intact crystals have been previously reported and are shown for comparison.[1] The curves in different colours for the ground crystals correspond to emission spectra measured at different points within the crystal.

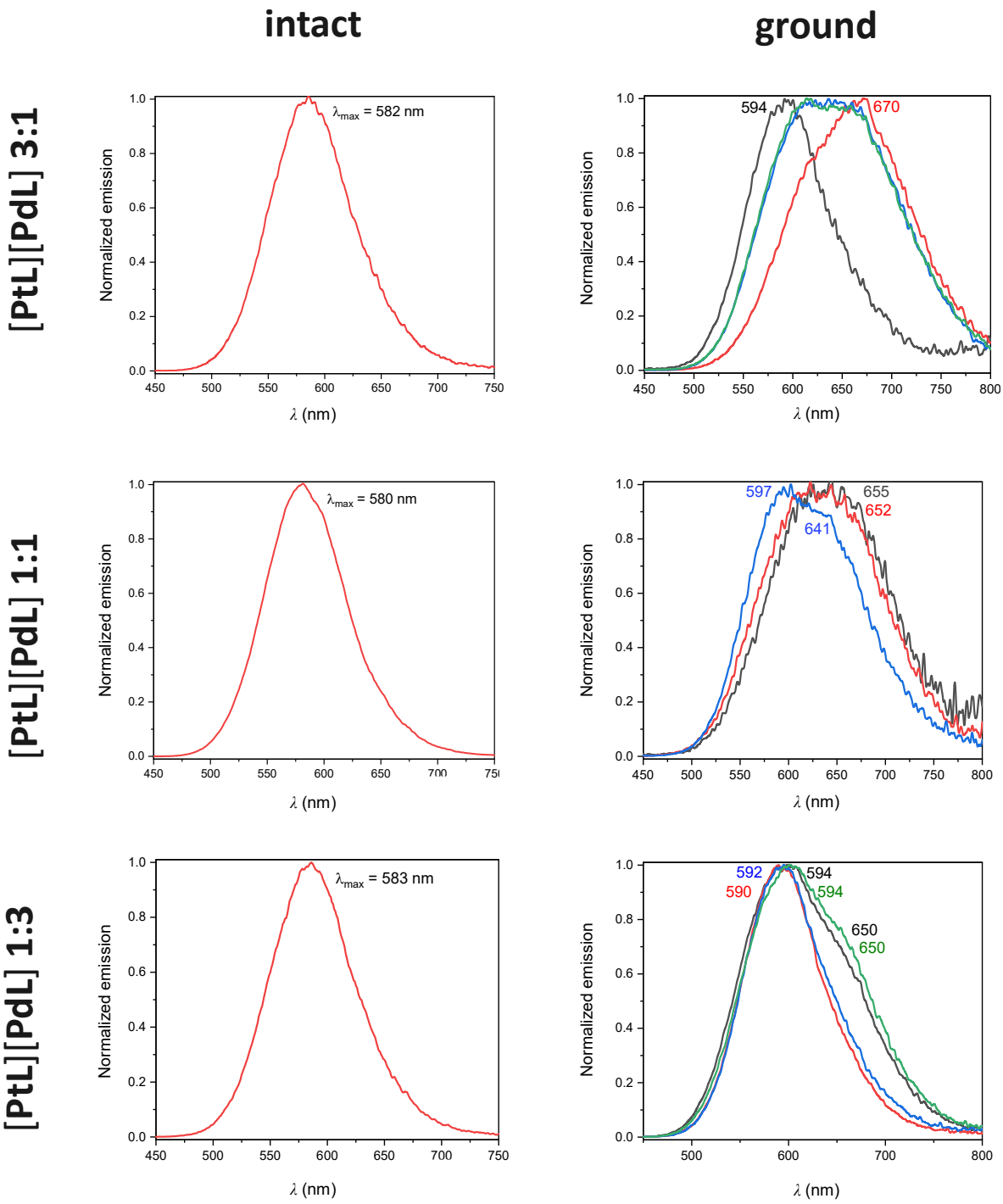

Fig. S17. Photoluminescence spectra (λ_{ex} = 375 nm) of the statistical co-crystals before (left) and after (right) mechanical grinding, as recorded by using time-resolved photoluminescence micro(spectro)scopy. The curves in different colours for the ground crystals correspond to emission spectra taken at different points within the crystal.

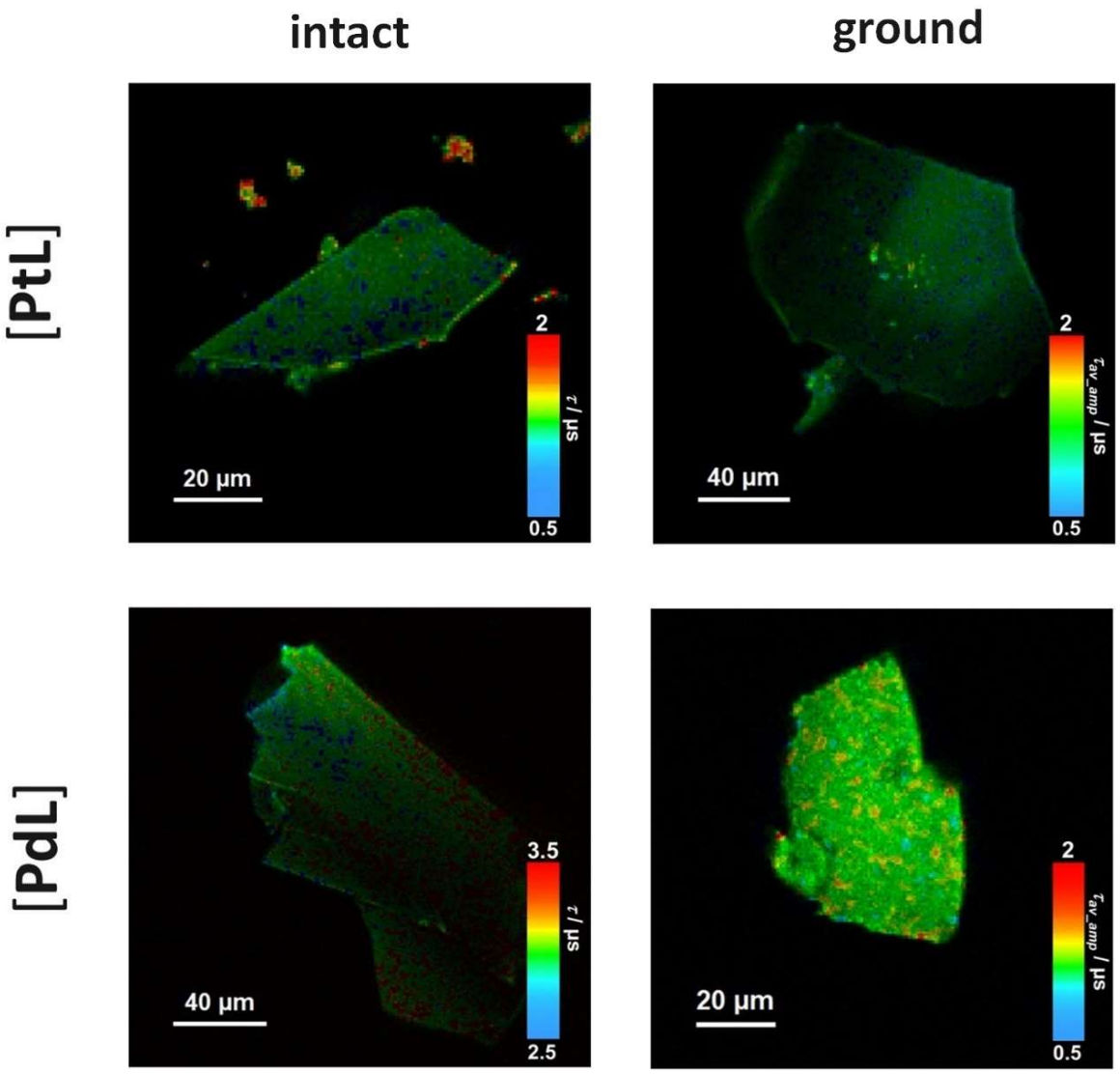

Fig. S18. Lifetime maps of the pure complexes [**PtL**] and [**PdL**] in the crystalline state before (left) and after (right) mechanical grinding, as recorded by using time-resolved photoluminescence micro(spectro)scopy. The maps of the intact crystals have been reported previously and are shown for comparison.[1]

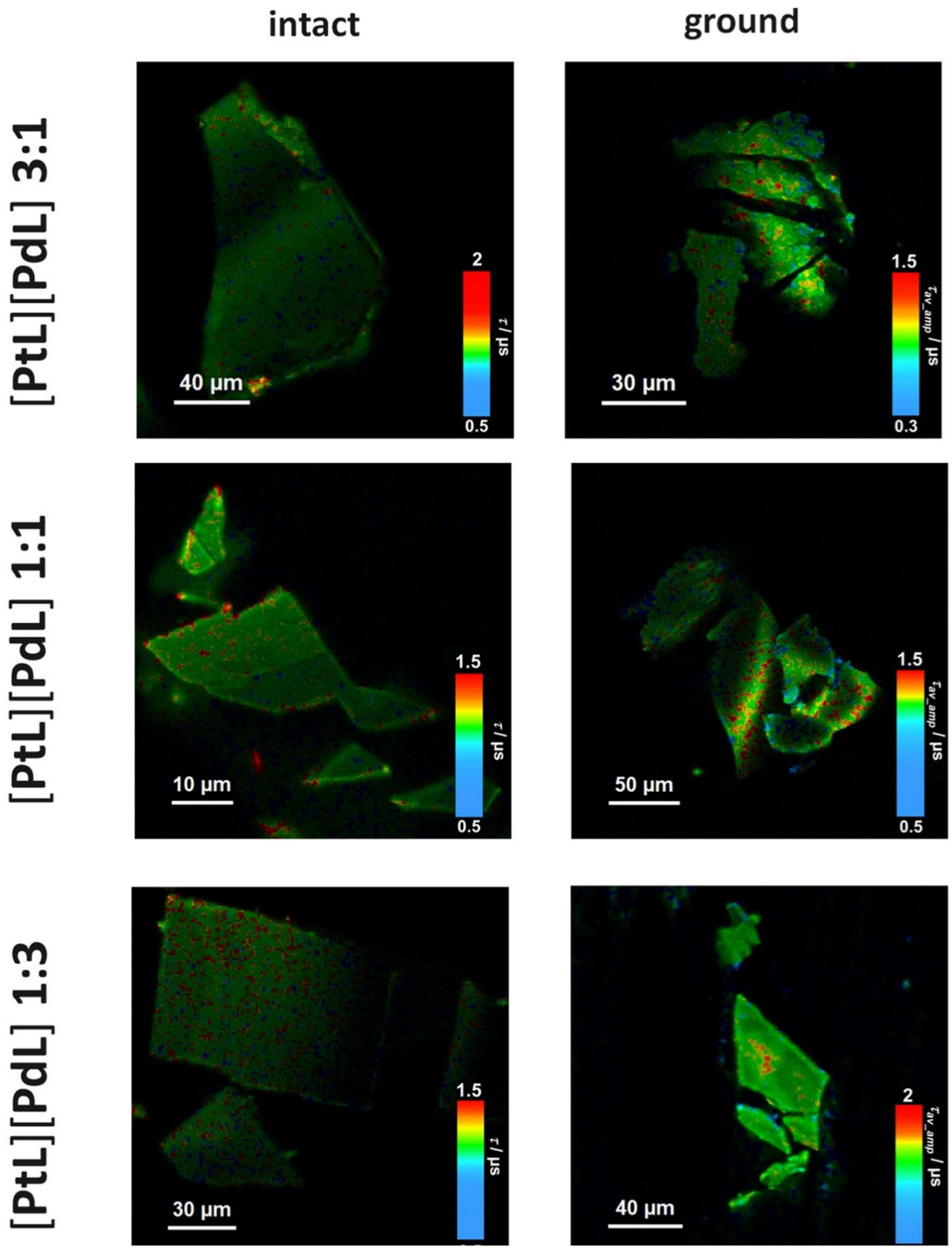

Fig. S19. Lifetime maps of the statistic heterobimetallic co-crystals in the crystalline state before (left) and after (right) mechanical grinding, as obtained by time-resolved photoluminescence micro(spectro)scopy.

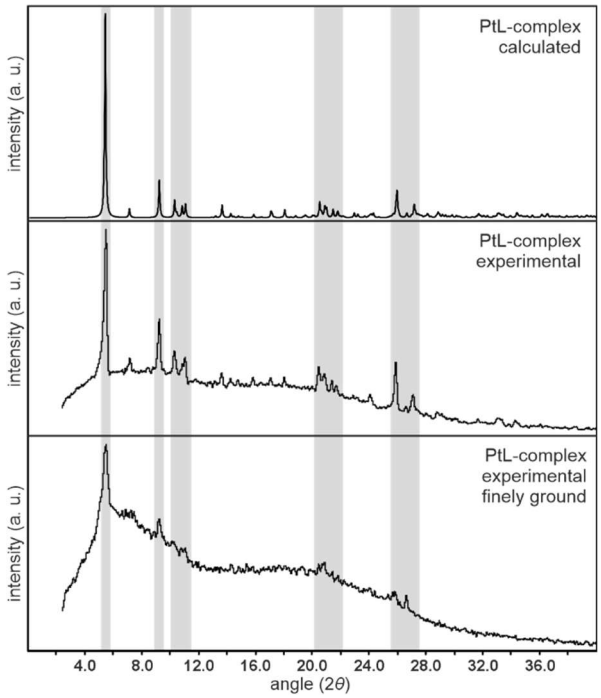

Fig. S20. X-ray powder diffractogram (CuK$_{\alpha 1}$ radiation) of [**PtL**]. Top: Calculated diffractogram of [**PtL**]. Centre: Diffractogram before grinding. Bottom: Diffractogram after grinding. The grey bars serve as a guide to the eye.

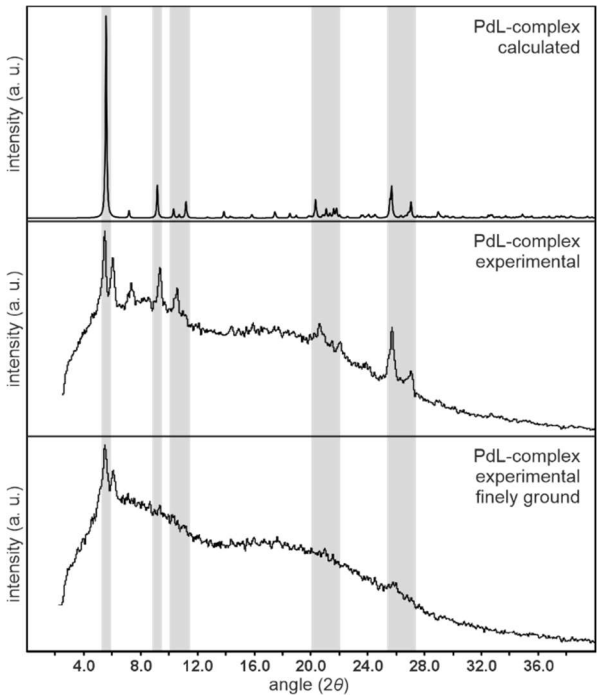

Fig. S21. X-ray powder diffractogram (CuK$_{\alpha 1}$ radiation) of [**PdL**]. Top: Calculated diffractogram of [**PdL**]. Centre: Diffractogram before grinding. Bottom: Diffractogram after grinding. The grey bars serve as a guide to the eye.

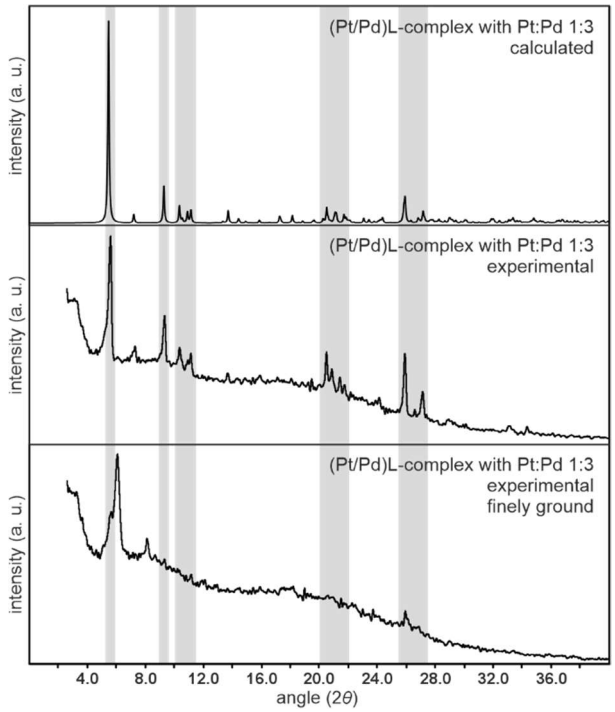

Fig. S22. X-ray powder diffractogram (Cu$K_{\alpha 1}$ radiation) of [**PtL**][**PdL**] 1:3. Top: Calculated diffractogram of [**PtL**][**PdL**] 1:3. Centre: Diffractogram before grinding. Bottom: Diffractogram after grinding. The grey bars serve as a guide to the eye.

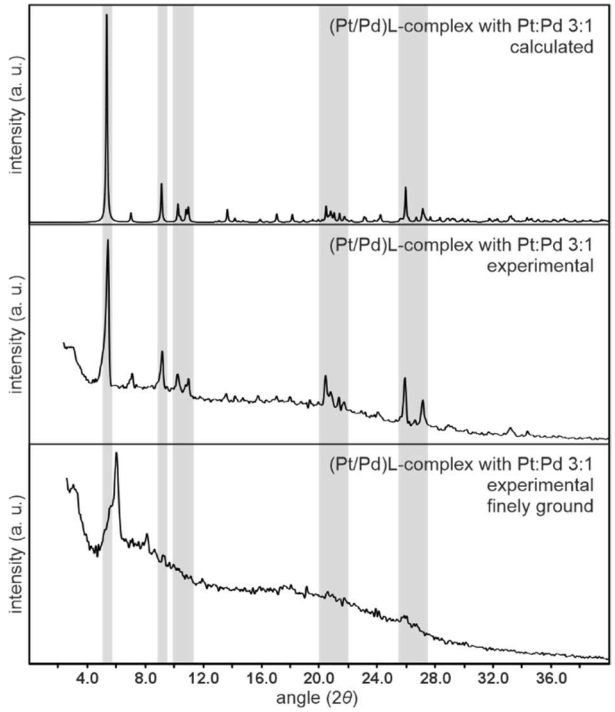

Fig. S23. X-ray powder diffractogram (Cu$K_{\alpha 1}$ radiation) of [**PtL**][**PdL**] 3:1. Top: Calculated diffractogram of [**PtL**][**PdL**] 3:1. Centre: Diffractogram before grinding. Bottom: Diffractogram after grinding. The grey bars serve as a guide to the eye.

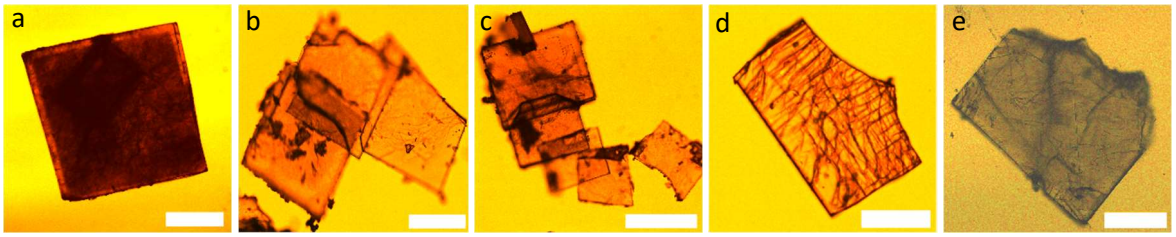

Fig. S24. Micrographs of the crystals observed under a bright-field microscope. **a)** [**PtL**]. **b)** [**PtL**][**PdL**] 3:1. **c)** [**PtL**][**PdL**] 1:1. **d)** [**PtL**][**PdL**] 1:3. **e)** [**PdL**]. Scale bar = 20 µm

Fig. S25. Images of the crystals taken with a normal camera. Left: [**PtL**]. Centre: [**PtL**][**PdL**] 1:1. Right: [**PdL**]. Scale bar = 60 µm.

Section S4: References

(1) T. Theiss, S. Buss, I. Maisuls, R. López-Arteaga, D. Brünink, J. Kösters, A. Hepp, N. L. Doltsinis, E. A. Weiss and C. A. Strassert, *J. Am. Chem. Soc.*, 2023, **145**, 3937–3951.

(2) *SAINT+* (includes *Xprep* and *SADABS*); Bruker AXS Inc., Madison, Wisconsin, USA, 2021.

(3) G. M. Sheldrick, *Acta Crystallogr.*, 2008, **A64**, 112–122.

(4) I. J. Bruno, J. C. Cole, P. R. Edgington, M. Kessler, C. F. Macrae, P. McCabe, J. Pearson and R. Taylor, *Acta Crystallogr.*, 2002, **B58**, 389–397.